Names Targeting p65 to Inhibit Cas3 Transcription by Onjisaponin B for Radiation Damage Therapy in p65+/- Mice

Tao-yang Wang
Rizhao People's Hospital,xinxiang medical university
Yong-jian Hu
Rizhao People's Hospital, xinxiang medical university
Xia Wang
Xinxiang Medical University
Yu-feng Li
Rizhao People's Hospital
Fan Zhang
Xinxiang Medical University
Yi-di Yan
Xinxiang Medical University
Wen-tao Dou
Xinxiang Medical University
Chen-yi Cheng
Xinxiang Medical University
Ping Xu (pingxu-zxsys@rz.shandong.cn)
Rizhao People's Hospital ,xinxiang medical university

Research

Keywords: Onjisaponin B, Radioprotection, NF-κB, p65, Caspase-3 , p65+/- mice, lung, thymus

Posted Date: August 3rd, 2021

DOI: https://doi.org/10.21203/rs.3.rs-754223/v1

Abstract

Background: p65 is activated following radiation injury. The formation of p65 is regulated by Onjisaponin B (OB) in Alzheimer's disease models. In addition, there is a binding site for p65 in the promoter region of CAS3. In the present study, the use of OB as an intervention to modulate p65/Cas3 following radiation injury was studied.

Methods: Cellular and animal experiments, immunofluorescence, HE staining, Western blotting, qRT-PCR, comet and DNA ladder assays, and flow cytometry were used to confirm the expression of p65 and Cas3.

Results: The results demonstrated that if the expression of p65 was silenced in V79 and TC cells, OB did not significantly inhibit the activation of p65 or Cas3 following irradiation, or significantly inhibit the phosphorylation of p65 and its transfer into the nucleus. Overexpression of p65 in V79 and MTEC-1 cells resulted in OB significantly inhibiting the activation of p65 and Cas3, and the phosphorylation and translocation of p65 into the nucleus. In p65+/- mice, expression of the p65 gene was knocked down, leading to increased tissue apoptosis and inflammation, and serious tissue pathological changes. The inhibition of p65 activation by OB after exposure to radiation was not apparent in the thymus, but it was in the lung, indicating that OB has a regulatory effect on endogenous p65.

Conclusions:

In summary, OB interfered with radiation injury by targeting and regulating p65/Cas3. Therefore, it was confirmed that p65 is an important target molecule for the treatment of radiation injury.

Background

Recent data suggested that the incidence of radiation-induced lung injury was highest when treating patients of lung cancer (5–25%), followed by mediastinal lymphoma (5–10%) and breast cancer (1–5%) [1–6] (Fig.S 1A). Understanding the mechanisms of radiation injury will assist in formulating protective treatments against radiation.

NF-κB is a nuclear transcription factor identified in 1986 by the Massachusetts Institute of Technology Cancer Research Center and the Massachusetts Institute of Biomedicine. It is a nuclear protein found in lymphocytes and in combination with immunoglobulin light chain, is closely associated with cell proliferation, apoptosis, inflammation, differentiation, and cycling [7, 8].

NF-κB is usually present in the cytoplasm along with IκBα, an inhibitor of the nuclear translocation of NF-κB. Activation of IKKβ leads to the phosphorylation of IκBα serine residues [9, 10]. IKKβ is a component of the inhibitor of κB (IκB) kinase (IKK) complex and its activation forms part of the key regulatory process that typically occurs in the NF-κB pathway [11]. Activation of the IKK complex invariably occurs when tissues are exposed to extracellular stresses such as radiation, inflammation, and reactive oxygen species [12]. Phosphorylated IκBα then becomes ubiquitinated and targeted for 26s proteasome degradation,

while NF-κB that has dissociated from IκBα enters into the nucleus and binds to DNA, resulting in the expression of genes of inflammatory and anti-apoptotic proteins, or cell-adhesion molecules [13–15]. Because NF-*κ*B becomes activated after exposure to radiation, a number of studies have identified substances targeting NF-*κ*B as radioprotection agents [16, 17].

Onjisaponin B (OB) is a saponin compound extracted from P. tenuifolia (Fig.S 1B). Our research group for the first time has revealed that it played a significant role in radio-protection using cellular and animal experiments (Fig.S 2A-E and S3), for which we have applied for a national patent as a therapy for radiation exposure [18]. NF-κB p65 formation is stimulated by lipopolysaccharide (LPS) in the hippocampus and the number of PC12 cells has been shown to increase due to LPS stimulation. Nevertheless, both have been shown to be significantly attenuated following OB treatment [19]. OB inhibits the expression of the p65 subunit of NF-κB in the nucleus and attenuates the expression of RhoA and ROCK2 proteins in a mouse model of Parkinson's disease [20]. In a model of inflammation, Tenuigenin B (a product of the hydrolysis of OB) was found to prevent an IL-1β-induced inflammatory response by inhibition of PI3K/AKT/NF-κB [21]. OB inhibits renal injury caused by LPS by inhibition of the NF-κB signaling pathway [22]. In addition, it has been identified that OB also inhibits osteoclast proliferation and reduces bone loss through down-regulation of NF-κB activity [23]. The molecular mechanisms of OB described above suggest that it may regulate NF-κB via PI3K/AKT. Therefore, a molecular mechanism by which OB acts is the regulation of NF-κB (in a non-radiation injury model). The mechanism of radioprotection by OB through inhibition of p65 remains to be defined.

Following radiation injury, both NF-κB and caspase-3 become activated, although their relationship is unknown. Current research has demonstrated that NF-κB activates caspase-3 in a model of neonatal retinal hypoxia, resulting in retinal ganglion cell death. NF-κB inhibitors inhibit caspase-3-dependent apoptosis [24]. Activation of NF-κB further activates caspase-3, and inhibition of NF-κB activation further suppresses caspase-3 activity [25]. It is apparent, therefore, that NF-κB activates the apoptosis-related molecule, caspase-3.

Taken together, we hypothesize that OB inhibits caspase-3 activation via NF-κB and protects against radiation damage (Fig.S 1C).

Materials And Methods

Materials

Plasmids of cDNA and shRNA of p65 (cDNA: 55304-1; shRNA: 5405-1, 5406-1, 5407-1) and Cas3 (cDNA: 55749-1; shRNA: 5402-1), and negative controls were purchased from Shanghai Jikai Gene Medical Technology Co., Ltd. (Shanghai, China). Primary antibodies against caspase-3 (19677-1-ap), p65 (10745-1-ap), GAPDH (10494-1-ap), and α-actinin (11313-2-ap) were purchased from Proteintech Group Inc. (Wuhan, China), while p-p65 antibody was purchased from Abcam (ab86299, Cambridge, UK). Secondary antibodies included goat anti-rabbit IgG labeled with Cy3 (A0516, Bi-Yun-Tian Biotechnology Co., Ltd, Shanghai, China) and horseradish peroxidase (HRP) (CST, 7074S, MA, USA). The following reagents were

used to quantify gene expression: RNAiso Plus reagent (Takara Bio Inc.), ReverTra Ace qPCR RT Master Mix kit (Toyobo Co., Ltd. Life Science Department, Osaka, Japan), and SYBR1 Green Real-time PCR Master Mix kit (Toyobo Co., Ltd.). A protease inhibitor cocktail was obtained from Roche Diagnostics GmbH (11836145001). All drug concentrations are expressed as final working concentrations in buffers. A bicinchoninic acid (BCA) assay kit was supplied by Bi-Yun-Tian Biotechnology Co., Ltd (P0010, Shanghai, China). Enhanced chemiluminescent (ECL) reagents were purchased from Bi-Yun-Tian Biotechnology Co., Ltd. (P0018AS, Shanghai, China).

Cell cultures

TC cells(thymocytes) were primary cell cultures prepared by our laboratory. V79 cells were obtained from the Chinese Academy of Sciences Cell Bank (CS0199) while MTEC-1 cells were purchased from Shanghai Hongshun Biological Technology Co., Ltd (HSC9942). All cell types were cultured in suspension in RPMI-1640 medium supplemented with 10% fetal bovine serum, 100 U/mL penicillin, and 100 U/mL streptomycin at 37°C in a humidified atmosphere containing 5% CO_2.

Irradiation

Cells were irradiated *in vitro* at room temperature at a dose rate of 100 cGy/min for a total dose of 6 Gy [26]. Cells in the treatment group were supplemented at concentrations of 20 μg/mL for 2 hours prior to irradiation.

For the *in vivo* studies, animals were placed in bespoke boxes [27] prior to exposure to 6 Gy of total body radiation at a dose rate of 100 cGy/min. OB was administered orally for 4 days at a dose of 2.5 mg/kg prior to irradiation. At various time points, the mice were sacrificed, tissue blocks were harvested and different physiological indicators were measured.

Quantitative real-time polymerase chain reaction (qRT-PCR)

Total RNA was extracted from 30-50 mg tissue using 1 mL RNAiso Plus reagent. The corresponding cDNA was created from 1 μg of the RNA from each sample using a ReverTra Ace qPCR RT Master Mix kit, in accordance with the manufacturer's instructions. The reaction system was heated to 37°C for 15 min, 50°C for 5 min, then 98°C for 5 min using BIO-RAD T100 Thermal Cycler. PCR product was diluted 10 times for qPCR. The reaction system was then heated to 95°C for 1 min, then taken through 40 cycles of heating to 95°C for 15 s, 60°C for 30 s and 72°C for 45s. The following primer sequences were used (mus/ham):

Caspase3-F: GGACTGATGAGGAGATGG, ATCGTGACACACACTGGACC;

Caspase3-R: AAAGGGACTGGATGAACC, CCATGAGACTGCAGCACAGA.

p65-F: GGACCTATGAGACCTTCAAGAG, GATGCGATTAGTTTTGGCTTCC;

p65-R: ACAGAAGTTGAGTTTCGGGTAGG, CCCGTGTAGCCATTGATCTGT

GAPDH-F: AGGTCGGTGTGAACGGATTTG and GAPDH-R: TGTAGACCATGTAGTTGAGGTCA. mRNA expression levels of the target genes were calculated relative to the endogenous control gene, GAPDH, using the $2^{-\Delta\Delta CT}$ method.

Western blotting

Cells were lysed using cell-lysis buffer (20 mM Tris-HCl, 2 mM EDTA, 137 mM NaCl, 1% NP-40, and 10% glycerol, with an aliquot of 1 mM PMSF and proteinase inhibitor cocktail added just prior to use). Lysis was conducted on ice for 30 min, with vortex mixing at 5 min intervals, after which the suspension was centrifuged at 12000 rpm for 15 min at 4°C. The tissue samples were homogenized on ice in cell-lysis buffer, as described above, except that lysis was conducted on ice for 45 min. The supernatant after centrifugation represented total tissue or cellular protein. The concentration was assayed using a BCA protein assay. A total of 40-80 μg protein was separated by SDS-PAGE after which the protein bands were transferred to a membrane. Each membrane was incubated with an appropriate dilution of a primary antibody (p65: 1;2000; p-p65: 1:1000; Cas3: 1:1000; GAPDH: 1:10000; or α-actinin: 1:2000), followed by incubation with horseradish peroxidase-conjugated secondary antibody diluted 1:2000. Protein bands were visualized using enhanced chemiluminescence (ECL). The intensity of bands on the Western blots was measured using ImageJ software. Background intensity was subtracted from each calculated band density.

Preparation and identification of p65+/- mice

C57BL/6J-Rela^{em1Smoc} mice (NM-KO-190139), referred to as p65+/- mice, were prepared by Shanghai Southern Model Biotechnology Co., Ltd, with transcript Ensembl number: Rela-201 ENSMUST00000025867.5. CRISPR/Cas9 technology was used to knock out exon 4 of the p65 gene and then non-homologous recombination was used to repair the introduced mutations, resulting in a frameshift of the Rela gene protein reading frame and loss of function (sgRNA1: GCCCCAGCAGACTTGCCTCCTGG; sgRNA2: GGCTGGCCTGTCCAGCCATAGGG)

A 0.1-0.2 cm section of mouse tail was placed into an EP tube and 60 μL of solution A(an alkaline lysis reagent: 25mM NAOH and 0.2mM disodium EDTA, pH 12 not adjusted) were added. The mouse tail was lysed for 30 minutes in a closed metal bath at 100°C. The lid was opened and excess pressure released every 5 minutes. The lysed mouse tail was flicked with a finger, then cooled to 4°C . An 80 μL aliquot of solution B (a neutralizing reagent: 40mM Tris-HCl, pH 5, not adjusted) was added to the EP tube which was then centrifuged to evenly mix the liquids at 10000 rpm for 5 min at 4°C, after which the supernatant was removed. PCR was then performed to confirm mouse tail gene transformation (P1: AGGGTGGGCACTGGAGTTTATTGA Common,

P2: GAGGCCCAGGGAAGGTGACAGAGA Mutant,

P3: GATGAGGCCGGTGAGGTGGAT Wildtype（WT）;

Mutant=846/997bp, WT =546bp).

Flow cytometry assays (FCM)

An Annexin V-FITC flow cytometry assay was used to detect cellular apoptosis. Cells were incubated with treatment drugs for 2 hours then irradiated with 6 Gy radiation. After different durations (TC cells: 6 h, V79 cells: 48 h, MTEC-1 cells: 24 h), the cells in each group were pelleted by centrifugation at 1800 rpm for 5 min, washed three times with cold PBS then gently resuspended in 195 μL Annexin V-FITC binding solution. An aliquot comprising 10 μL Annexin V-FITC and 5 μL propidium iodide (PI) dye was carefully added to the cells and incubated at room temperature for 15 min in the dark. Apoptosis was identified by flow cytometry (FCM) as green fluorescence, cell death was represented by red and green fluorescence, while living cells emitted no fluorescence.

Immunohistochemistry

Harvested tissue was fixed in 4% paraformaldehyde overnight, processed, then embedded in paraffin. The tissue blocks were then sliced into 4μm-thick sections and placed on polylysine-treated slides, and dewaxed by placing in xylene prior to incubation through a gradient of alcohol concentrations. The sections were then placed in a 0.01M sodium citrate solution at pH 6.0 for antigen retrieval and cells were permeabilized by treatment with 0.3% Triton X-100 for 20 min. Non-specific staining was blocked by placing the slides in a humid container and incubating with 10% sheep serum for 60 min at room temperature. The slides were then incubated with primary antibody (1:200) overnight at 4°C, then with Cy3-labelled secondary antibody (1:500) in a humid chamber at room temperature for 1 h, washing with PBS after each incubation. The slides were incubated with DAPI for 2 minutes at room temperature then rinsed 3 times in PBS for 3 min each time. An anti-fluorescent quencher was added to the tissue sections in the dark. The fluorescence of tissue sections was imaged using Pannoramic a MIDI digital slide scanner (3DHISTECH).

Histological analysis of tissue

Paraffin sections were deparaffinized and stained with hematoxylin and eosin, dehydrated, then mounted with neutral gum. Finally, the sections were examined using a Pannoramic MIDI digital slide scanner (3DHISTECH).

Staining of tissue with Hoechst

Paraffin sections were placed in an oven at 60°C and warmed for 30 minutes, then a small volume of Hoechst 33342 staining solution was added to cover the samples and incubated for 5 min. The Hoechst 33342 staining solution was then aspirated off the slides which were washed in PBS 3 times, 5 min each

time. The stained slides were then directly observed using an inverted fluorescence microscope. The nuclei of cells undergoing apoptosis were densely stained.

Statistical analysis

Data were expressed as means ± standard deviation (SD). The data were analyzed by analysis of variance (ANOVA) using SPSS/PC* (statistical package for social sciences, personal computer) and ImageJ software. The group means were compared using a Duncan's Multiple Range Test (DMRT). The means of the treated groups were compared with those of the radiation-alone or non-irradiated groups. A value of $P < 0.05$ was considered statistically significant.

Results

Effects of OB on p65-induced cas3 transcription activation after silencing p65 following exposure radiation

p65 protein was significantly phosphorylated 2 h after irradiation, and the Cas3 protein was significantly sheared 14 h after irradiation in V79 cells (Fig. 1A, B). Compared with the radiation group, the expression levels of the activation products p-p65 and c-Cas3 in the OB 20 μg/mL treatment group were significantly down-regulated, differences were statistically significant (Fig. 1C). A p65 knockdown model was established in V79 cell cultures (Fig. 1D). After transfection of the p65 shRNA plasmid, the ability of 20 μg/mL OB intervention to down-regulate the expression of p-p65 and c-Cas3 proteins was significantly reduced, or even reversed (Fig. 1E, F). In addition, Cas3 mRNA expression was also down-regulated after transfection with p65 shRNA. Compared with the untransfected group, the ability of the drug group to down-regulate Cas3 mRNA was also inhibited or even reversed, as displayed in Fig. 1G. The observations above indicated that OB regulated Cas3 transcription through p65 and affected protein expression, thereby reducing injury from radiation.

p65 protein molecules in TC cells were significantly phosphorylated 1 h after irradiation while Cas3 proteins were significantly cleaved 6 h after irradiation (Fig.S 4A, B). The effect of OB on TC cells after irradiation (Fig.S 4C, D), and its regulation of cas3 following transfection with p65 shRNA was consistent with that observed in V79 cells, as displayed in Fig.S 4E-H. The data above demonstrated that OB inhibited the activation of Cas3 through p65, thereby reducing radiation-induced cell apoptosis and thus helping to prevent radiation injury.

Effects of OB on the nuclear translocation of p65 after silencing p65 following exposure to radiation

After exposure to irradiation, p65 in V79 cells became activated, its expression increased and it transferred from the cytoplasm to the nucleus. Here, p65 translocation to the nucleus was monitored at different time points after irradiation. It was found that the greatest level of nuclear translocation occurred 8 h after irradiation (Fig. 2A). OB inhibited the activation of p65 and its transfer into the nucleus after irradiation. After transfection with p65 shRNA, the transfer of p65 into the nucleus was inhibited. Compared with plasmid transfection without the addition of OB, the inhibition of transfer of p65 into the nucleus in cells treated with OB and in which the plasmid had been transfected was not apparent (Fig. 2B). Therefore, the effect of OB was not clear, indicating that OB protected cells from radiation injury by inhibiting the transfer of p65 into the nucleus.

After TC cells were transfected with the p65 shRNA plasmid, the same changes occurred as those observed in V79 cells (Fig.S 5).

Effect of OB on cell apoptosis after silencing caspase3 with irradiation

A Cas3 knockdown model was established in V79 cells (Fig. 2C). As shown in panel D, OB inhibited activation of Cas3 following exposure to the radiation, reducing the production of c-Cas3. After V79 cells were transfected with Cas3 shRNA plasmid, Cas3 expression was significantly down-regulated. The flow cytometry results indicated that, compared with the radiotherapy group alone, OB reduced apoptosis caused by radiotherapy. Moreover, the down-regulation of Cas3 expression after transfection with Cas3 shRNA plasmid reduced apoptosis caused by radiation. Compared with the Cas3 shRNA plasmid transfection group, the effect of OB on cell apoptosis caused by radiation following plasmid transfection was not significant, as shown in Fig. 2E.

The same changes were observed in TC cells following transfection with the Cas3 shRNA plasmid as observed in V79 cells (Fig.S 5).

The data above indicated that OB inhibited activation of Cas3 through p65, thus reducing radiation-induced cell apoptosis and preventing radiation injury.

Effect of OB on p65-induced cas3 activation and p65 nuclear translocation following p65 overexpression due to radiation exposure

MTEC-1 thymic epithelial cells are a purified subpopulation of TC cells. They grow adherently and are easily transfected with large fragments of overexpression plasmids. The p65 protein became significantly phosphorylated 1 h after irradiation, while the Cas3 protein was significantly sheared 8 h after irradiation, as shown in Fig.S 6A. V79 and MTEC-1 cells were transfected with p65 overexpression plasmids, as

displayed in Fig. 3A, B and S 6B. Compared with the p65 overexpression plasmid group, significantly reduced expression of p-p65 and c-Cas3 were still observed in the OB administration group, a difference that was statistically significant. As displayed in Fig. 3C and S 6C, compared with the p65 overexpression plasmid transfection group, after plasmid transfection, OB administration also inhibited activation of phosphorylation caused by radiation and transfer of p65 into the nucleus.

Effect of OB on cell apoptosis following overexpression of caspase3 due to radiation

As displayed in Fig. 4A, B and S 7A, compared with the Cas3 overexpression plasmid transfection group, OB administration following plasmid transfection had no significant effect on inhibition of Cas3 shear-activation. As shown in Fig. 4C, D and S 7B, in V79 cells analyzed by flow cytometry and Hoechst staining 2 d and 3 d after irradiation, in addition to MTEC-1 cells 24 h after irradiation, compared with the Cas3 plasmid overexpression transfection group, administration of OB following plasmid transfection still caused a difference in the reduction of apoptosis, whereas the reduction in apoptosis in V79 cells 3 days after radiation and after 24 hours in MTEC-1 cells was not significant.

Preparation of mice

p65+/- mice were designed and prepared by Shanghai Southern Model Biotechnology Co., Ltd. (Fig. 5A). Preliminary genetic identification of the model mice was performed following receipt, after which co-cage breeding was conducted. The p65 DNA fragment was partially cut off (CRISPR/Cas9 system), gene amplification generating a 997/846 bp fragment. Because of the one-sided knockout, the mouse was heterozygous (Fig. 5B).

Down-regulation of p65 gene led to increased inflammation and apoptosis in p65+/- mice

Three days after irradiation, the p65 protein in lung tissue was clearly activated (Fig. 6A). Six days after irradiation, the integrity of the lung tissue of radiation-injured mice was severely reduced, with a significant increase in alveolar interstitium, which caused a decrease in the volume of alveoli (Fig. 6B). Three days after irradiation, the Cas3 protein in lung tissue was clearly activated (Fig. 6C). Six days after irradiation, apoptosis of tissue cells increased significantly after radiation (Fig. 6D). For p65+/- mice, compared with WT mice, because of the down-regulation of p65 gene, inflammation and apoptosis were both increased (Fig. 6E-G).

In WT mice, three days after irradiation, Cas3 in the thymus tissue was significantly activated (Fig.S 8A). Six days after irradiation, apoptosis of tissue cells increased significantly after radiation (Fig.S 8B). Two hours after radiation, p65 protein was significantly activated (Fig.S 8C). 6 days after irradiation, the integrity of the thymus tissue was severely reduced, with an unclear boundary between cortex and medulla and tissue displayed a diffuse arrangement(Fig.S 8D). For p65+/- mice, compared with WT mice,

because of the down-regulation of p65 gene, Inflammatory damage to tissue structure and apoptosis were both increased (Fig. S 8E-F).

OB inhibited p65 and cas3 activation caused by p65, and significantly reduced pathological changes and apoptosis (caused by down-regulation of p65) and the nuclear translocation of p65 in the lung tissue of p65+/- mice following radiation, but not in the thymus

The results indicated that in WT mice, compared with the radiation group, the protein expression levels of p-p65 and p65 in the 2.5 mg/kg OB intervention group was significantly reduced after irradiation, differences were statistically significant. For p65+/- mice, compared with WT mice, the ability of 2.5 mg/kg OB intervention to down-regulate protein of p-p65 expression was significantly reduced (Fig. 7A B). Administration of OB reduced injury caused by radiation, with the lungs of the mice maintaining normal morphology, with fewer pathological changes in the mouse lung. In p65+/- mice, due to partial loss of p65, the tissues of irradiated mice produced significantly more alveolar interstitium, which was more severe than in WT mice. Intervention with OB changed the response to injury (Fig. 7C).

In WT mice, compared with the radiation group, the protein expression levels of Cas3 and c-Cas3 and Cas3 mRNA in the 2.5 mg/kg OB intervention group was significantly reduced after irradiation, differences were statistically significant. For p65+/- mice, compared with WT mice, the ability of 2.5 mg/kg OB intervention to down-regulate protein of c-Cas3 expression was significantly reduced (Fig. 7D-F). Hoechst staining of tissue cell apoptosis demonstrated that compared with the p65+/- mouse irradiation group, administration of OB group had a different effect on inhibiting tissue cell apoptosis, as shown in Fig. 7G. Immunofluorescence analysis demonstrated that compared with untreated irradiated p65+/- mice, p65 was regulated differently in irradiated p65+/- mice that received OB, as presented in Fig. 7H.

In p65+/- mice, compared with the radiation group, 2.5 mg/kg intervention with OB down-regulated levels of p-p65, there were no significant difference between the two groups (Fig.S 9A). OB reduced the damage caused by radiation and maintained normal morphology of the thymus tissue, thereby preventing pathological changes to the mouse thymus. In p65+/- mice, due to the partial loss of p65, the structure of the tissue in the non-irradiated group was slightly diffuse, then the morphology was severely disrupted following irradiation. The ability of OB to reduce post-irradiation injury was significantly inhibited such that the difference between the two groups was not significant (Fig.S 9B). For the protein expression levels of Cas3, c-Cas3 and Cas3 mRNA, it is the same as p-p65 (Fig.S 9C D). Hoechst staining of cell apoptosis demonstrated that compared with the irradiated p65+/- mice, no significant inhibitory effect on tissue cell apoptosis in the OB group was observed, as shown in Fig.S 9E. In the thymus tissue,

immunofluorescence analysis demonstrated that compared with the irradiated p65+/- mice group, there was no apparent regulatory effect on p65 in the p65+/- mouse irradiation group (Fig.S 9F).

In summary, in mouse thymus tissue, OB reduced splicing activation of Cas3 by inhibition of p65 phosphorylation and reduced radiation injury.

Discussion

The present study is the first to identify inhibition of NF-κB-dependent caspase-3 activation by OB and to demonstrate the role of NF-κB/caspase-3 in an intervention using OB against radiation injury.

In the present study, we further demonstrated that OB reduced radiation injury via p65. There is binding site for NF-κB in the Caspase-3 promoter region in mice (Fig.S 10). For the first time, we have provided evidence that OB protected against radiation injury via regulation of Cas3 by p65. This finding not only revealed a novel mechanism of action of OB, it also suggested a basis for the identification of target drugs for radiation protection.

We confirmed the expression of p65 in TC, V79, and MTEC-1 cells, and p65+/- mice at various time points following exposure to radiation, recording the dynamic changes in their expression after irradiation, as well as the regulation of p65 by OB. NF-κB is a member of the Rel family, consisting of homodimers or heterodimers of p50 and p65 subunits, and plays a major role in the regulation of heterodimers. At rest, IκB binds to NF-κB in the cytoplasm as a trimer and inhibits its activity. When stimulated by exogenous sources (*e.g.*, ionizing radiation, TNF-α), IκB kinase (IKK) phosphorylates IκB. IκB is then phosphorylated and degraded, while NF-κB is activated, after which it enters the nucleus and binds to specific target sites to regulate gene expression [28, 29]. Studies have shown that ROS produced by oxidative stress can induce IκB activation [30] (Fig.S 11). In contrast, ROS scavengers inhibit NF-κB activation and nuclear translocation [31]. Therefore, oxidative stress can induce NF-κB activation. Ionizing radiation is also an activator of the NF-κB pathway. It has been reported that NIH/3T3 cells can be activated by irradiation, which caused an intracellular oxidative stress response and activation of NF-κB [32]. It has been reported that naringin inhibited γ-ray-induced DNA damage and inflammation in mouse spleen cells by regulating p53 and the NF-κB signaling pathway [33]. Tetramethylpyrazine was shown to inhibit radiation-induced lymphocyte apoptosis by downregulation of NF-κB in the cytoplasm [34]. NF-κB expression in astragalus polysaccharide-pretreated mice was found to be significantly lower than in a radiation-only group [35]. Therefore, it has been established that the radiation injury model was closely associated with the activation of NF-κB. In the present study, we found that TC cells were more sensitive to radiation than lung fibroblasts in terms of p65 activation. The time required for p65 to become activated in TC, V79, and MTEC-1 cells after irradiation was 1h, 2h, and 1h, respectively (Fig. S4A, 1A, and S6B). For TC cells, phosphorylation and nuclear translocation of p65 occurred 1h after irradiation, but for V79 and MTEC-1 cells, nuclear translocation occurred 8h and 6h after irradiation, respectively (Fig.S 5A, 2 and S 6E).

The present study also demonstrated that activation of CAS3 by p65 is a common mechanism at the initial stage of radiation injury, and that OB inhibited the activation of CAS3 via p65. Interestingly, where

p65 was knocked down, the activation of Cas3 was significantly reduced, and regulation of Cas3 by OB via p65 was not apparent (Fig. 1 and S4).

In the case of p65 overexpression, CAS expression was significantly increased, while administration of OB nevertheless partially reduced the expression of CAS3, because OB downregulated the overexpression of activated p65 (Figs. 3 and S6). In addition, following overexpression of Cas3, OB did not significantly regulate CAS3 expression. By overexpressing both p65 and CAS3, it was observed that OB regulated Cas3 in V79, and MTEC-1 cells via p65 (Figs. 4A and S7A). We bred model mice in which exon 4 of p65 was knocked down. The results of the *in vivo* studies indicated that for p65+/- mice, the protein and mRNA expression levels of p-p65 and c-Cas3 were not significantly down-regulated by 2.5 mg/kg OB intervention compared with the irradiation group in mouse thymus tissue, with no significant differences between the two groups (Fig. 6 and S8). In lung tissue, different regulation was observed, supporting the hypothesis that the effect of OB on Cas3 is dependent on p65. The results also indicate that OB also inhibited endogenous p65 activation after p65 knockdown, further inhibiting Cas3 activation. We have previously reported that radiation injury is mediated by caspase-3/PARP-1 [36]. The caspase-3 inhibitor Z-VAD-FMK significantly inhibits activation of caspase-3 following irradiation and prevents apoptosis [36, 37]. Therefore, radiation injury is also closely associated with the activation of caspase-3. Thus, we hypothesize that p65 may be upstream of Cas3/PARP1 in the pathway following radiation injury.

Conclusions

In summary, the present study identified a common mechanism by which radiation induces damage to organisms.There is a binding site for p65 in the promoter region of Cas3. When radiation occurs, p65 could be recruited to the promoter region of Cas3 where it enhanced Cas3 transcription. OB, an active component of saponin, inhibited the activation of p65 and the activation of Cas3 gene caused by p65 following exposure to radiation, resulting in reduced apoptosis and protection against radiation injury. p65/Cas3 may serve as prognostic biomarkers and promising therapeutic targets forradiation damage.

Abbreviations

Abbreviations	Full name
OB	Onjisaponin B
TC	Thymus cells
WT	Wild type
NF-κB p65	Nuclear factor-kappaB p65
p-p65	Phosphorylated p65
Cas3	Caspase-3
c-Cas3	Cleaved-Caspase3
OD	Optical Density
PBS	Phosphate Buffered Saline
mRNA	messenger RNA
PI	Propidium iodide
SDS	Sodium Dodecyl Sulphate
ECL	Enhanced Chemiluminescence
HE	Hematoxylin-eosin staining
Tris	Tri-(hydroxymethyl)-Aminomethane
PCR	Polymerase Chain Reaction
DNA	Deoxyribonucleic acid
RNA	Ribonucleic Acid
SPSS	Stastical package for social science

Declarations

Acknowledgements

We thank Dr. Shuagnxi Wang for his kind help on the initiation of this research.

Authors' contributions

Ping Xu designed and performed experiments, analyzed data and wrote the paper. Tao-yang Wang and Yong-jian Hu performed experiments and analyzed the data. They contribute equally. Xia Wang, Yu-feng Li, Fan Zhang, Yi-di Yan, Wen-tao Dou, and Chen-yi Cheng performed some of the experiments. All authors read and approved the final manuscript.

Funding

This work was supported by the National Science Foundation of China (NSFC) (Nos. 81773358, 11705158, U1504824) and the Young Teachers Plan of Higher Schools in Henan Province (2014GGJS-098).

Availability of data and materials

Datasets used and/or analyzed during the current study are available from the corresponding author on reasonable request.

Ethics approval and consent to participate

The present study was approved by the Experimental animal ethics committee of Xinxiang Medical University.

Consent for publication

Not applicable.

Competing interests

The authors declare that they have no competing interests.

Author details

1 Radiology Laboratory, Central laboratory, Rizhao people's Hospital, 276800

2 Henan Key Laboratory of Medical Tissue Regeneration Xinxiang Medical University, Xinxiang, Henan, 453003, China

3 College of Medical Laboratory, Xinxiang Medical University, Xinxiang 453003, Henan, China

4 Basic Medical school, Xinxiang Medical University, Xinxiang, Henan, 453003, China

References

1. Marks LB, Bentzen SM, Deasy JO, et al. Radiation Dose–Volume Effects in the Lung. Int J Radiat Oncol , 2010, 76(3):S70-S76.
2. Tsoutsou PG, Koukourakis MI. Radiation pneumonitis and fibrosis: Mechanisms underlying its pathogenesis and implications for future research. Int J Radiat Oncol, 2006, 66(5):1281-1293.
3. Ebert N, Baumann M, Troost EGC. Radiation-induced lung damage-Clinical risk profiles and predictive imaging on their way to risk-adapted individualized treatment planning? Radiother Oncol, 2015, 117(1):1-3.

4. Marks L, Yu X, Vujaskovic Z, et al. Radiation induced lung injury. Semin Radiat Oncol, 2003, 13(3):333-345.
5. Mehta V. Radiation pneumonitis and pulmonary fibrosis in non-small-cell lung cancer: Pulmonary function, prediction, and prevention. Int J Radiat Oncol , 2005, 63(1):5-24.
6. Pinnix CC, Smith GL, Milgrom S, et al. Predictors of radiation pneumonitis in patients eceiving intensity modulated radiation therapy for Hodgkin and non-Hodgkin lymphoma. Int J Radiat Oncol Biol Phys , 2015, 92(1):175–182.
7. Visekruna A, Volkov A, Steinhoff U. A key role for NF- κB transcription factor c-Rel in Tlymphocyte-differentiation and effector functions. Clin Dev Immunol, 2012:239368.
8. Rayet B, Gélinas C. Aberrant rel/nfkb genes and activity in human cancer. Oncogene, 1999, 18:6938-6947.
9. Oida KA, Matsuda K, Jung et al. Nuclear factor-κB plays a critical role in both intrinsic and acquired resistance against endocrine therapy in human breast cancer cells, Scientific Reports, 2015, 4(1):4057
10. Hiscott J, Kwon H, Génin P. Hostile takeovers: viral appropriation of the NF-κB pathway. Clinical Investigation, 2017, 107(2):143-151.
11. Perkins ND. Integrating cell-signalling pathways with NF-κB and IKK function. Nature Reviews Molecular Cell Biology, 2007, 8(1): 49-62.
12. Janus PK, Szołtysek G, Zając et al. Pro-inflammatory cytokine and high doses of ionizing radiation have similar effects on the expression of NF-κB-dependent genes. Cellular Signalling, 2018, 46:23-31.
13. Lennikov AM , Hiraoka A, Abe et al . IκB kinase β inhibitor IMD-0354 beneficially suppresses retinal vascular permeability in streptozotocin-induced diabetic mice. Investigative Ophthalmology & Visual Science, 2014, 55(10): 6365-6373.
14. Verstrepen L, Beyaert R. Receptor proximal kinases in NF-κB signaling as potential therapeutic targets in cancer and inflammation. Biochemical Pharmacology, 2014, 92(4):519-529.
15. Panwalkar AS, Verstovsek, Giles F. Nuclear factor-κB modulation as a therapeutic approach in hematologic malignancies. Cancer, 2004, 100(8): 1578-1589.
16. Kengo Waga1, Masaru Yamaguchi1, Shuta Miura1 et al. IKK β Inhibitor IMD-0354 Attenuates Radiation Damage in Whole-body X-Irradiated Mice. Oxid Med Cell Longev , 2019:5340290.
17. Tiancong Wu1, Wen Liu , Ting Fan et al. Androstenediol prevents radiation injury in mice by promoting NF-κB signaling and inhibiting AIM2 inflammasome activation. Biomed Pharmacother , 2019. 109597.
18. Xu P, Zhang WB, Xiong XW. Application of Tenuigenin B in preparation of ionizing radiation protection drugs. Patent application No. 201610560668.0, Publication No: CN106176783A, Application Announcement Date: 2016.12.07.
19. Xinyu Li , Sun Yu , Yafen Wei, et al. Onjisaponin B (OB) is Neuroprotective During Cognitive Loss Through Immune-mediated and SIRT1 Pathways. Curr Neurovasc Res, 2018, 15(2):94-102.

20. Fang Peng , Linyu Lu , Fei Wei et al. The onjisaponin B metabolite tenuifolin ameliorates dopaminergic neurodegeneration in a mouse model of Parkinson's disease. Neuroreport, 2020, 31(6):456-465.
21. Wang C, Zeng L, Zhang T, et al . Tenuigenin Prevents IL-1β-induced Inflammation in Human Osteoarthritis Chondrocytes by Suppressing PI3K/AKT/NF-κB Signaling Pathway. Inflammation , 2016 , 39(2):807-812.
22. Fu H, Hu Z , Di X, et al. Tenuigenin exhibits protective effects against LPS-induced acute kidney injury via inhibiting TLR4/NF-κB signaling pathway. Eur J Pharmacol, 2016, 791:229-234.
23. Yang S , Li X , Cheng , Let al. Tenuigenin inhibits RANKL-induced osteoclastogenesis by down-regulating NF-κB activation and suppresses bone loss in vivo. Biochem Biophys Res Commun, 2015, 466(4):615-621.
24. Rathnasamy G , Sivakumar V, Rangarajan P , et al. NF-κB-mediated nitric oxide production and activation of caspase-3 cause retinal ganglion cell death in the hypoxic neonatal retina. Invest Ophthalmol Vis Sci , 2014, 55(9):5878-5889.
25. Cao ZH, Yin WD, Zheng QY, et al. Caspase-3 is involved in IFN-γ-and TNF-α-mediated MIN6 cells apoptosis via NF-κB/Bcl-2 pathway. Cell Biochem Biophys , 2013, 67(3):1239-48.
26. Mohan S , Abdelwahab SI , Kamalidehghan B , et al. Involvement of NF-κB and Bcl2/Bax signaling pathways in the apoptosis of MCF7 cells induced by a xanthone compound Pyranocycloartobiloxanthone A. Phytomedicine, 2012, 19:1007-1015.
27. Lui JC , Kong SK. Heat shock protein 70 inhibits the nuclear import of apoptosis-inducing factor to avoid DNA fragmentation in TF-1 cells during erythropoiesis. FEBS Lett ,2007, 581(1):109-117.
28. Ahmed KM, Li JJ.NF-kappa B-mediated adaptive resistance to ionizing radiation. Free Radic Biol Med. 2008, 44(1):1-13.
29. Viatour P, Merville MP, Bours V, et al. Phosphorylation of NF-κB and IκB proteins: implications in cancer and inflammation. Trends Biochem Sci , 2005, 30(1):43-52.
30. Morgan MJ , Liu ZG. Crosstalk of reactive oxygen species and NF-κB signaling. Cell Res, 2010, 21(1):103-115.
31. Kim DH, Lee JH, Park S, et al. 6-Acetonyl-5,6-dihydrosanguinarine (ADS) from Chelidonium majus L. triggers proinflammatory cytokine production via ROS-JNK/ERK-NFκB signaling pathway. Food Chem Toxicol, 2013, 58: 273-279.
32. Lam RK, Han W, Yu KN. Unirradiated cells rescue cells exposed to ionizing radiation: Activation of NF-κB pathway in irradiated cells. Mutat Res, 2015, 782:23-33.
33. Manna K, Das U, Das D, et al. Naringin inhibits gamma radiation-induced oxidative DNA damage and inflammation, by modulating p53 and NF-κB signaling pathways in murine splenocytes. Free Radic Res, 2015, 49(4):422-439.
34. Wang XY, Ma ZC, Wang YG, et al. Tetramethylpyrazine protects lymphocytes from radiationinduced apoptosis through nuclear factor-κB. Chin J Nat Med, 2014, 12(10): 0730-0737.

35. Liu Y, Liu F, Yang Y, et al. Astragalus polysaccharide ameliorates ionizing radiation-induced oxidative stress in mice. Int J Biol Macromol, 2014, 68:209-214.
36. Xu P, Cai XH, Zhang WB, Li YN, Qiu PY. Flavonoids of Rosa roxburghii Tratt exhibit radio-protection and anti-apoptosis properties via the Bcl-2(Ca2+)/Caspase-3/PARP-1 pathway. Apoptosis, 2016, 21(10):1125-1143.
37. Li J, Lin L, Du L, et al. Radioprotective effect of a pan-caspase inhibitor in a novel model of radiation injury to the nucleus of the abducens nerve. Mol Med Rep, 2014,10(3):1433-1437.

Figures

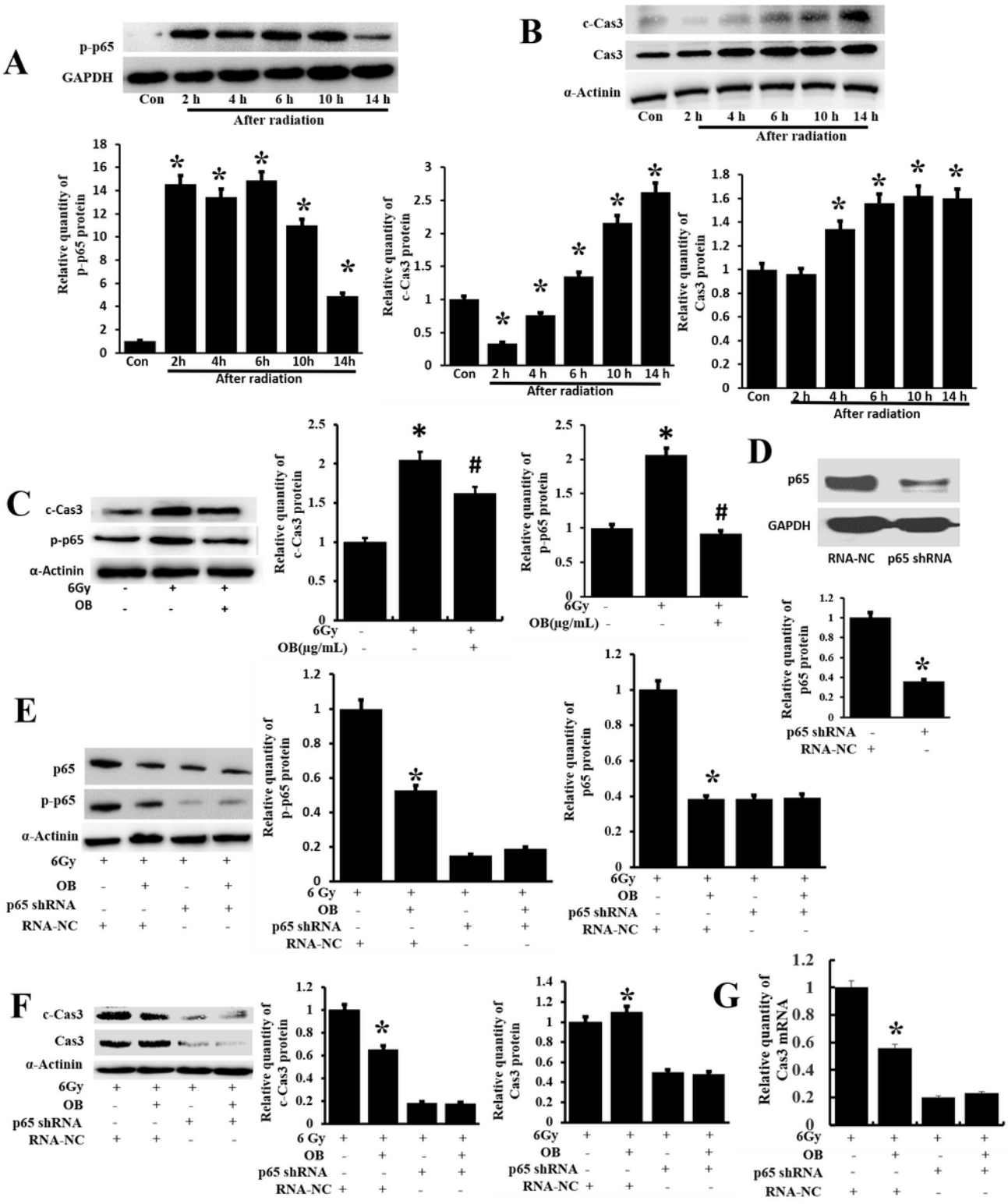

Figure 1

Effect of OB on the expression of p65 and Cas3 in V79 cells following irradiation, with p65 shRNA intervention. (A) Optimization of the measurement time points for p65 protein in V79 cells after irradiation. *Compared with the blank control group, p<0.01. (B) Optimization of the measurement time points for Cas3 protein in V79 cells after irradiation. *Compared with the blank control group, p<0.01. (C) Effect of OB on the expression of p-p65 and c-Cas3 protein in V79 cells after irradiation. *Compared with

the normal group, p<0.01; #Compared with the radiation group, p<0.01. (D) p65 shRNA results in p65 knockdown. *Compared with the negative control group, p<0.01. (E) Effect of OB on the expression of p65 protein in V79 cells after irradiation, with p65 shRNA intervention. *Compared with the radiation group, p<0.01. (F) Effect of OB on the expression of Cas3 protein in V79 cells following irradiation, with p65 shRNA intervention. *Compared with the radiation group, p<0.01. (G) Effect of OB on mRNA expression levels of Cas3 in V79 cells after irradiation, with p65 shRNA intervention. *Compared with the radiation group, p<0.01.

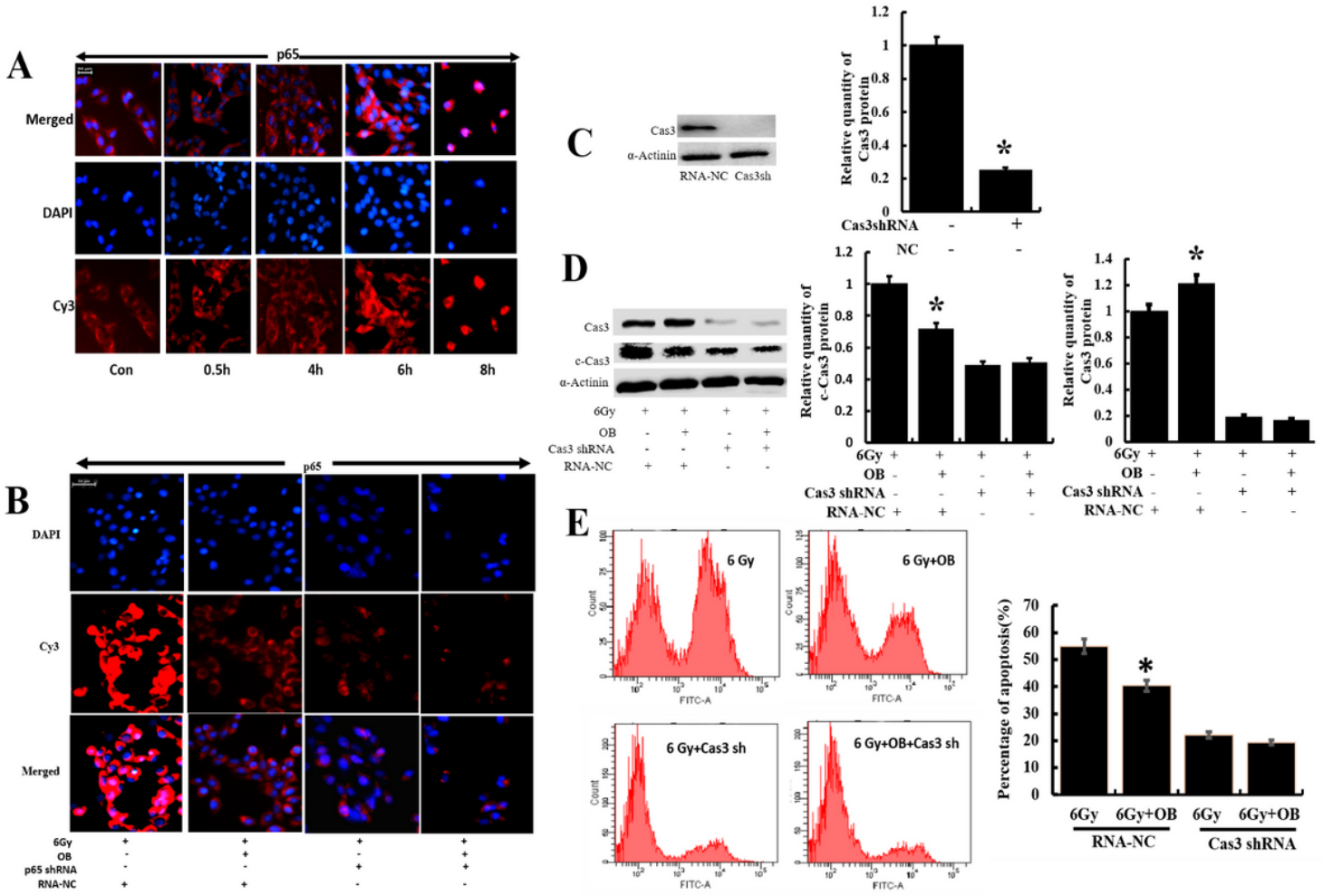

Figure 2

Effect of OB on the nuclear translocation of p65 and apoptosis caused by Cas3 after irradiation of V79 cells, with intervention by p65 shRNA. (A) Optimization of the measurement time points for p65 nuclear translocation in V79 cells after irradiation. (B) Effect of OB on the nuclear metastasis of p65 in V79 cells after irradiation, with p65 shRNA intervention. (C) Successful construction of Cas3 knockdown model in V79 cells. *Compared with the negative control group, p<0.01. (D) Effect of OB on the protein expression levels of Cas3 and c-Cas3 in V79 cells after Cas3 shRNA intervention. *Compared with radiation group p<0.01. (E) Effect of OB on the apoptosis of V79 cells after Cas3 shRNA intervention. *Compared with the radiation group, p<0.01.

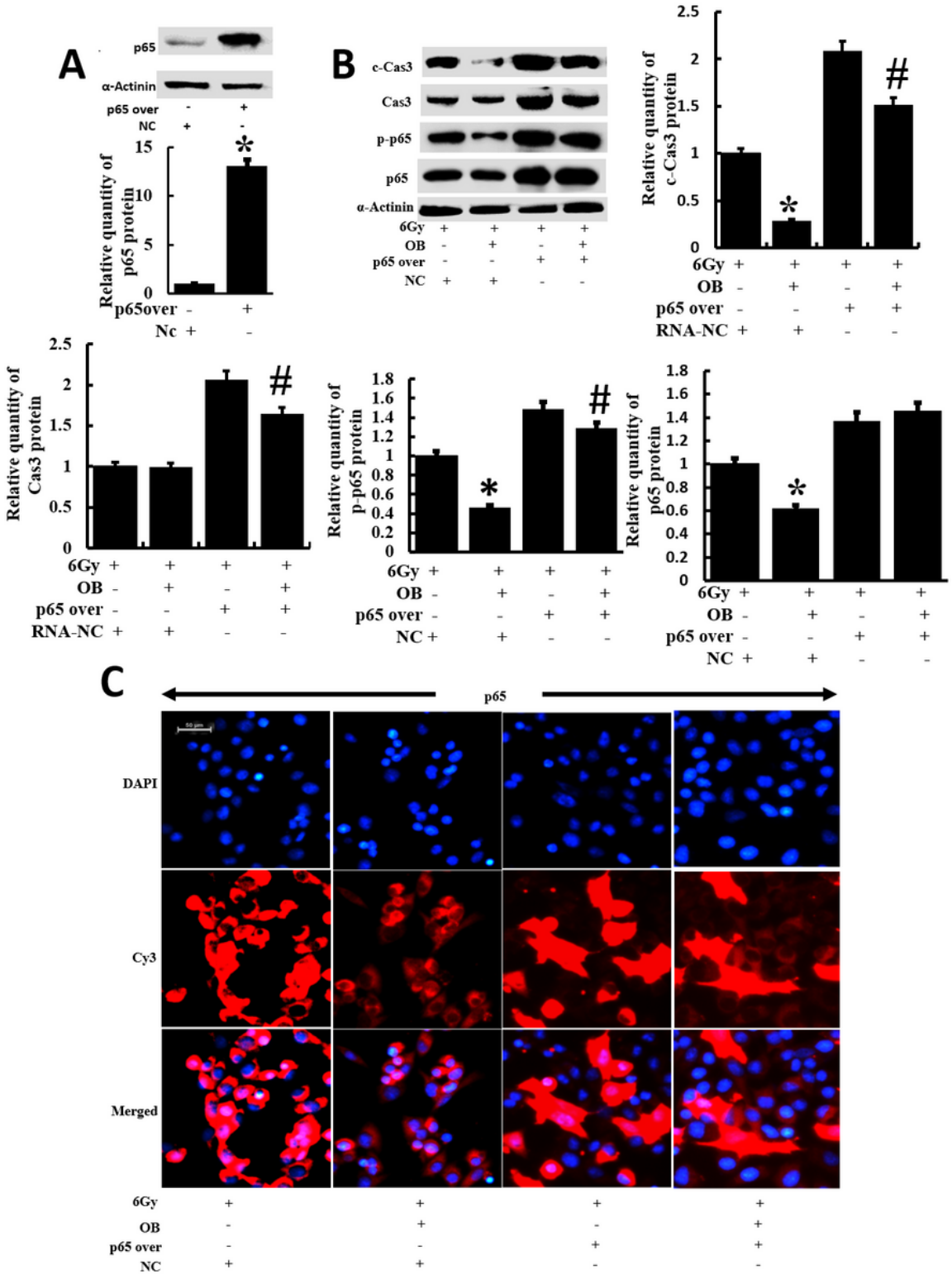

Figure 3

Effect of OB on protein expression levels of Cas3 and p65, and nuclear translocation after radiation of V79 cells, with p65 overexpression. (A) Preparation of p65 overexpression model of V79 cells. *Compared with the negative control group, p<0.01; (B) Effect of OB on Cas3 and p65 protein expression levels after irradiation of V79 cells, with p65 overexpression. *Compared with the radiation group, p<0.01; #Compared

with the radiation transfection group, p<0.01. (C) Effect of OB on the nuclear translocation of p65 protein after irradiation of V79 cells, with p65 overexpression.

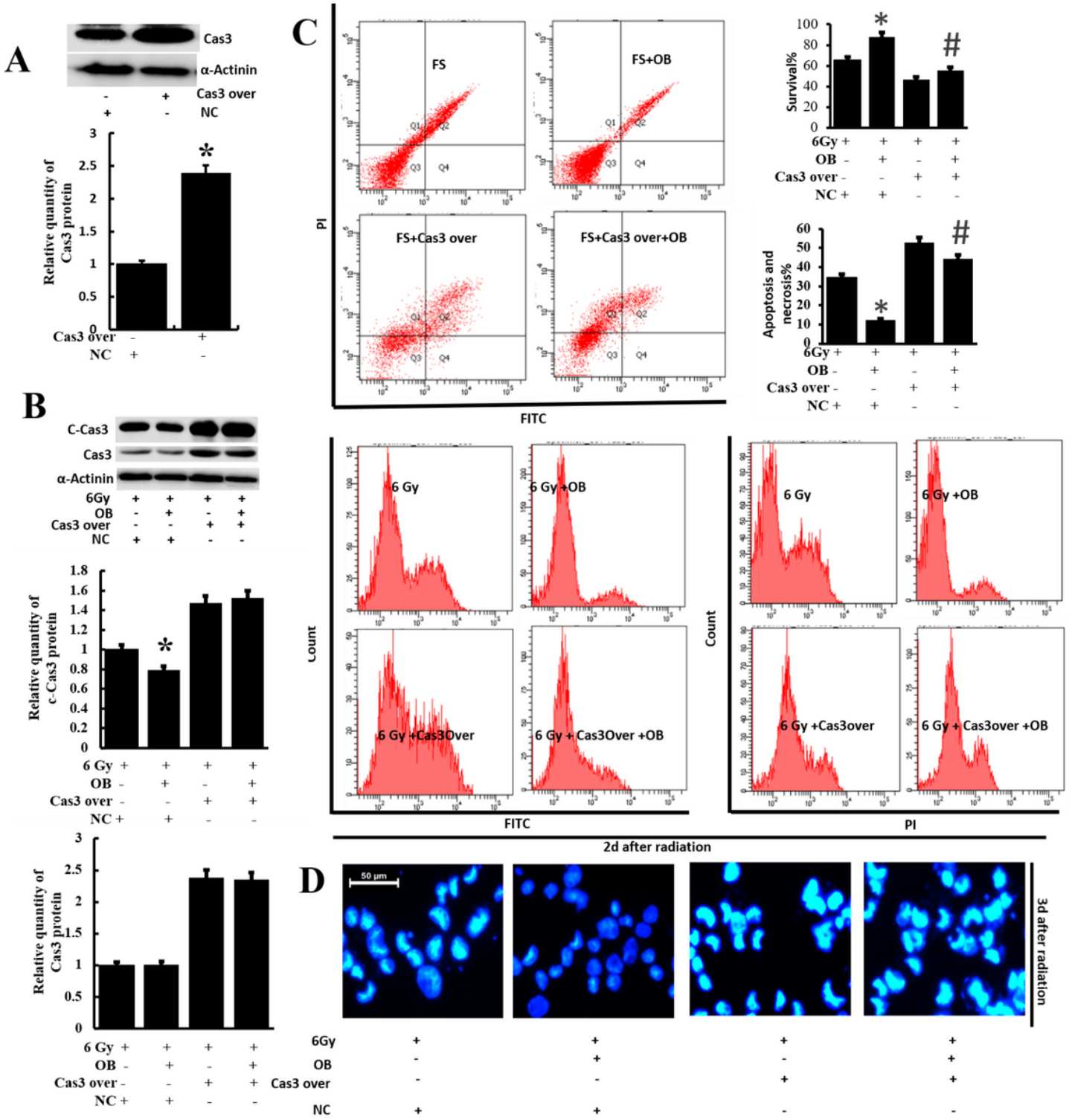

Figure 4

Effect of OB on Cas3 and cell apoptosis after radiation of V79 cells, with Cas3 overexpression. (A) Preparation of Cas3 overexpression model of V79 cells. *Compared with the negative control group, p<0.01. (B) Effect of OB on Cas3 protein expression levels after irradiation of V79 cells, with Cas3

overexpression. *Compared with the radiation group, p<0.01. (C) Effect of OB on the apoptosis of V79 cells, with Cas3 overexpression, after irradiation (Hoechst staining). (D) Effect of OB on the apoptosis of V79 cells, with Cas3 overexpression (Flow cytometric analysis). *Compared with the radiation group, p<0.01, #Compared with irradiated transfected Cas3 overexpression plasmid group, p<0.01.

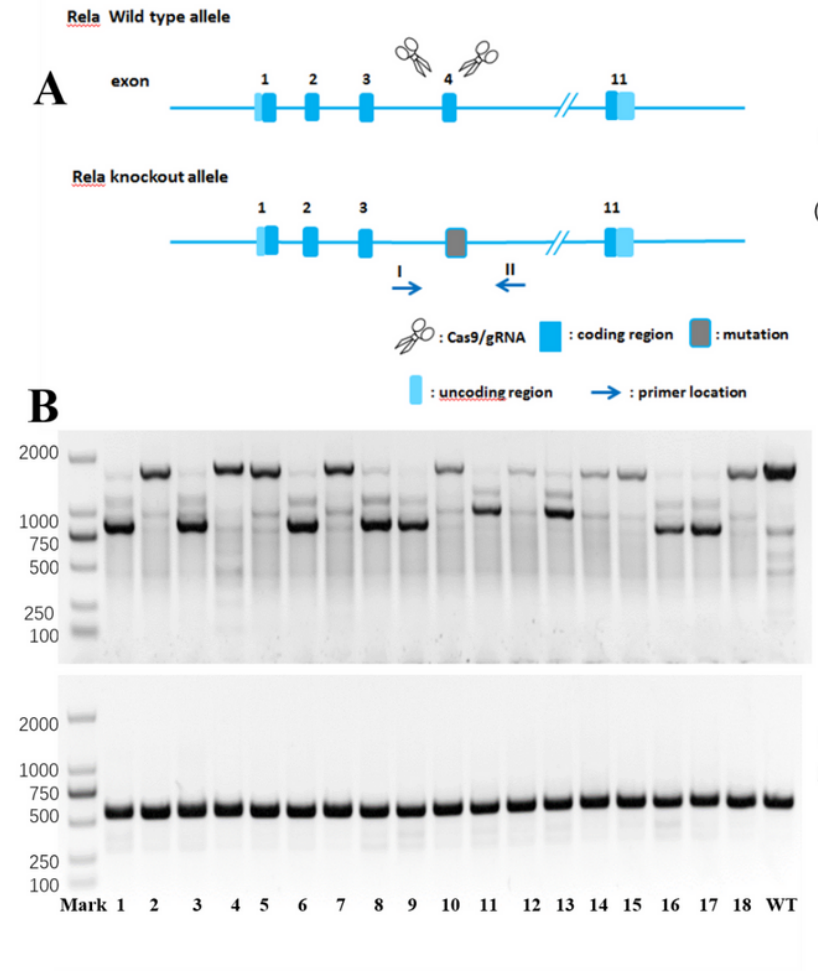

C57BL/6J-*Rela*^{em1Smoc}

Transcript number (Ensembl) : Rela-201 (ENSMUST00000025867.5) ;

Exon: exon 4

gRNA	Sequence (5'-3')
gRNA1	gccccagcagacttgcctcc tgg
gRNA2	ggctggcctgtccagccata ggg

Primer	Sequence (5'→3')	Primer Type
P1	AGGGTGGGCACTGGAGTTTATTGA	Common
P2	GAGGCCCAGGGAAGGTGACAGAGA	Mutant
P3	GATGAGGCCGGTGAGGTGGAT	Wild type

P1P2: WT=1637 bp, Mutant=997/846 bp; P1P3: WT=546 bp

p65+/- mice: 1\3\6\8\9\11\13\16\17; WT mice: 2\4\5\7\10\12\14\15\18

Figure 5

Design and gene identification of p65+/- mice. (A) Design of p65+/- mice. (B) Genetic identification of p65+/- mice.

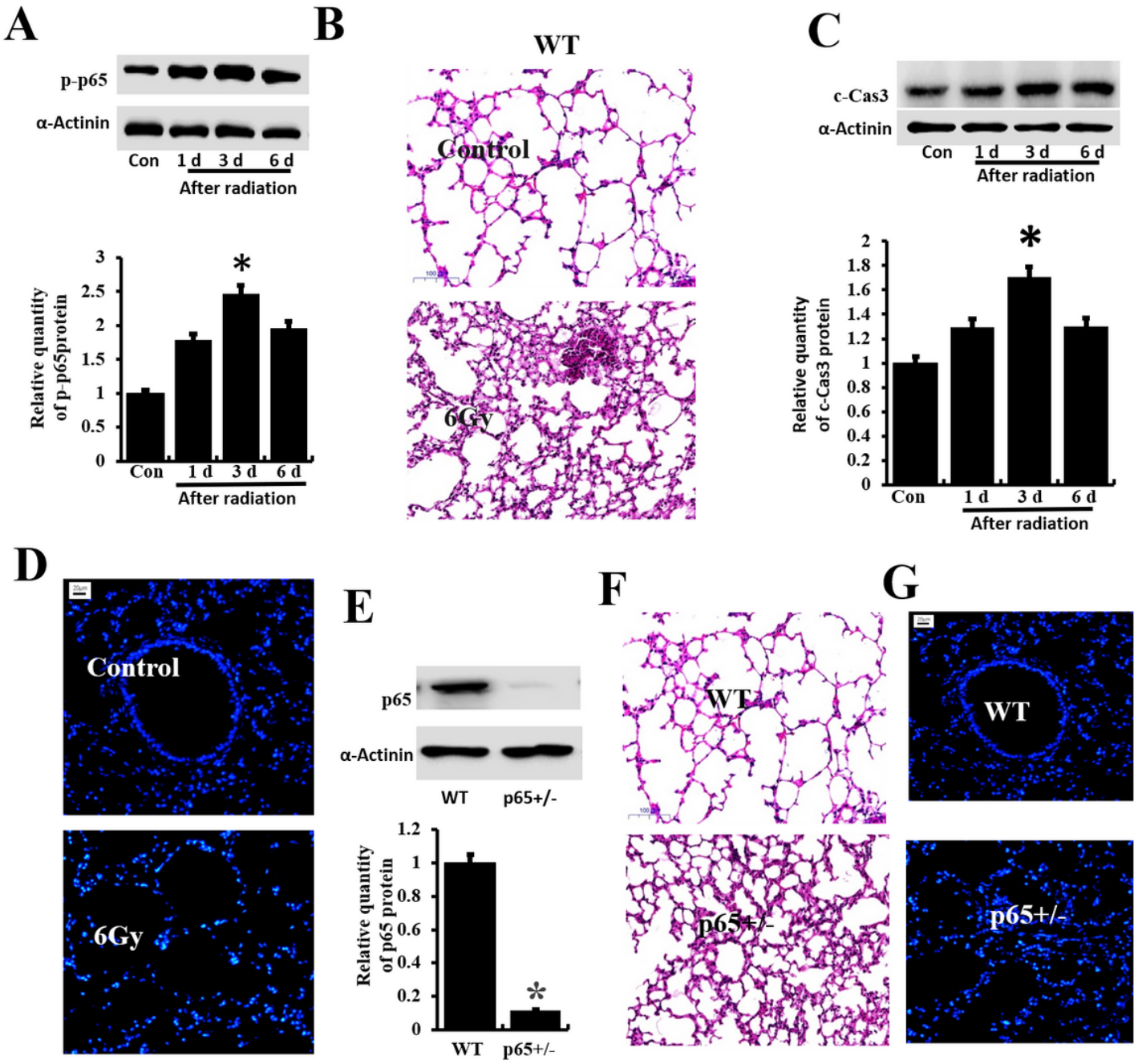

Figure 6

Down-regulation of p65 gene led to increased inflammation and apoptosis of lung tissue in p65+/- mice. (A) Optimization of the measurement time points for p65 protein expression in lung tissue following radiation. *Compared with the normal group, p□0.01. (B) Pathological changes to lung tissue in WT mice after radiation. (C) Optimization of the measurement time points for Cas3 protein expression in lung tissue following radiation. *Compared with the normal group, p□0.01. (D) Lung tissue apoptosis after irradiation of WT mice. (E) Measurement of p65 expression in p65+/- model mice. *Compared with the normal group, p<0.01. (F) Compared with WT mice, the tissue inflammatory damage was more serious in p65+/- mice. (G) Compared with WT mice, the tissue apoptosis was more serious in p65+/- mice.

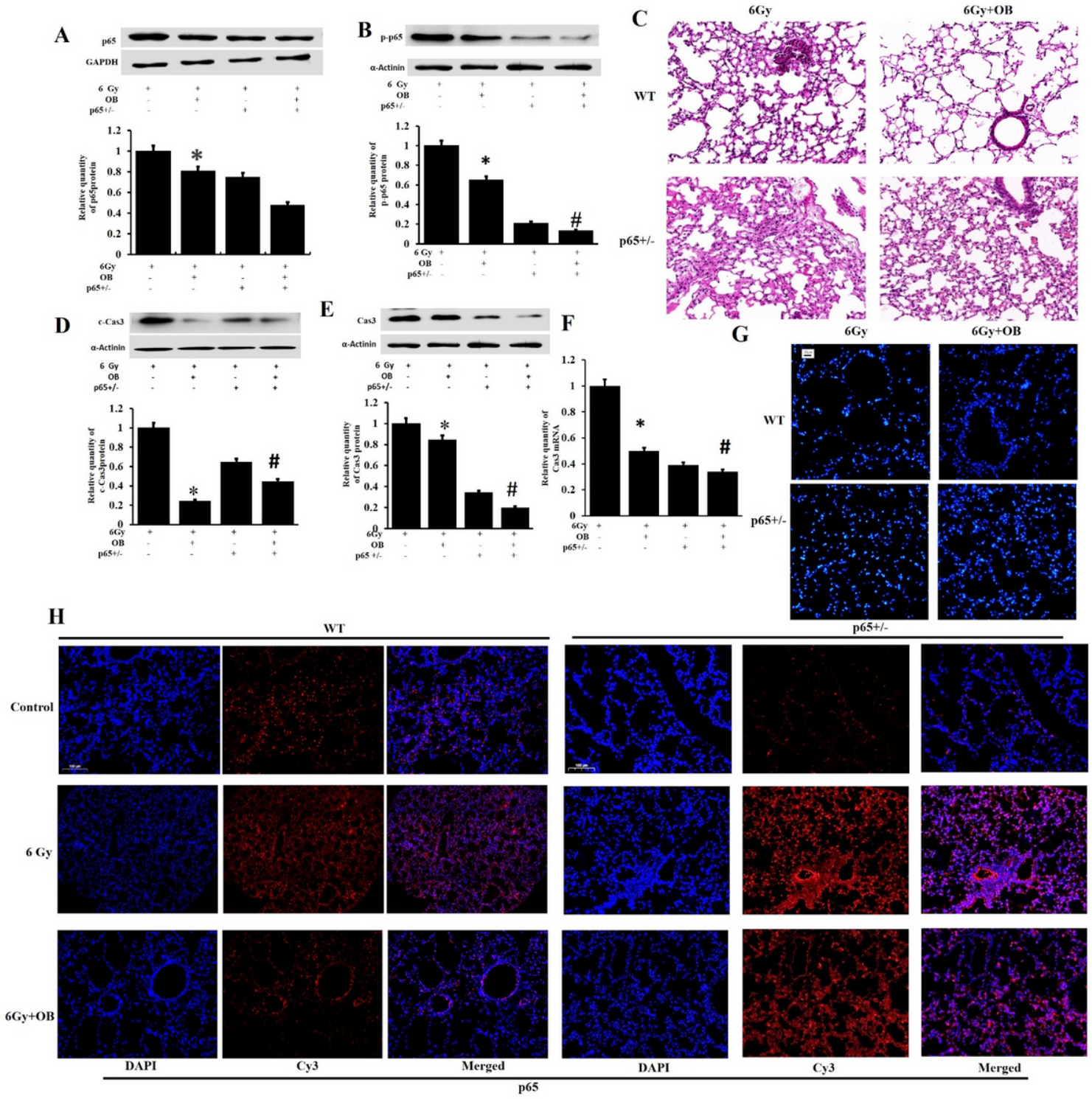

Figure 7

OB inhibited p65 activation and cas3 activation caused by p65, and accordingly reduced pathological changes and apoptosis (caused by down-regulation of p65) and the nuclear translocation of p65 in the lung tissue of p65+/- mice following radiation (A) Effect of OB on p65 protein expression in the lung tissue of p65+/- mice after irradiation. *Compared with the radiation group of WT mice, p<0.01. (B) Effect of OB on p-p65 protein expression in the lung tissue of p65+/- mice after irradiation. *Compared with the radiation group of WT, p<0.01; #Compared with the radiation group of p65+/- model mice, p<0.01. (C)

Effect of OB on pathological changes to lung tissue in p65+/- mice after radiation.(D) Effect of OB on c-Cas3 protein expression in the lung tissue of p65+/- mice after irradiation. *Compared with the radiation group of WT mice, p<0.01; #Compared with the radiation group of p65+/- model mice, p<0.01.(E) Effect of OB on Cas3 protein expression in the lung tissue of p65+/- mice after irradiation. *Compared with the radiation group of WT mice, p<0.01; #Compared with the radiation group of p65+/- model mice, p<0.01. (F) Effect of OB on Cas3 mRNA expression levels in the lung tissue of p65+/- mice after radiation. *Compared with the radiation group of WT mice, p<0.01; #Compared with the radiation group of p65+/- model mice, p<0.01. (G) Effect of OB on lung tissue apoptosis after irradiation of p65+/- mice. (H) Effect of OB on p65 translocation in the lung tissue of p65+/- mice after irradiation.

Supplementary Files

This is a list of supplementary files associated with this preprint. Click to download.

- supplementarydata.docx